

Dissipative quantum transport at arbitrary parameter regime: a variational method

Yu Zhang,^{1,*} ChiYung Yam,^{2,1} YanHo Kwok,¹ and GuanHua Chen^{1,†}

¹*Department of Chemistry, The University of Hong Kong, Pokfulam Road, Hong Kong*

²*Beijing Computational Science Research Center, No. 3 He-Qing Road, Beijing 100084, China*

(Dated: October 8, 2018)

Recent development of theoretical method for dissipative quantum transport have achieved notable progresses in the weak or strong electron-phonon coupling regime. However, a generalized theory for dissipative quantum transport at arbitrary parameter regime is not figured out until now. In this work, a variational method for dissipative quantum transport at arbitrary electron-phonon coupling regime is developed by employing variational polaron theory. The optimal polaron transformation is determined by the optimization of the Feynman-Bogoliubov upper bound of free energy. The free energy minimization ends up with an optimal mean-field Hamiltonian and a minimal interaction Hamiltonian. Hence, second-order perturbation can be applied to the transformed system, resulting an accurate and efficient method for the treatment of dissipative quantum transport with arbitrary electron-phonon coupling strength. Numerical benchmark calculation on a single site model with coupling to one phonon mode is also presented.

PACS numbers: 73.23.-b, 71.38.-k, 72.10.Bg, 73.63.-b

I. INTRODUCTION

Quantum transport and energy dissipation in nanostructures have been of great interest, which requires the study and understanding of nonequilibrium phenomena of open quantum systems.¹⁻⁶ In many previous studies on dissipative quantum transport, the coupling between the system and the phonon bath can be small. In this case, second-order perturbation (2PT) can be employed, leading to a set of equation of motions (EOM).⁶ However, there are many open quantum systems with strong electron-phonon coupling. For instance, the coupling between system and bath in the energy transfer process in photosynthetic complexes is comparable to the electronic coupling;⁷⁻⁹ Strong electron-phonon coupling is also observed in resonant tunneling in molecular transport junctions.^{10,11} Even though there are several non-perturbative methods to evaluate the dynamics numerically exactly, such as hierarchical equations of motion (HEOM),^{12,13} quasi-adiabatic propagator path integral (QUAPI)¹⁴ and multiconfiguration time-dependent Hartree (MCTDH) approach,¹⁵⁻¹⁷ these methods are computational demanding and not trivial to be implemented.

There is another group of methods to deal with strong electron-phonon coupling, which makes use of polaron transformation. A polaron transformed second-order master equation for open quantum system has been developed accordingly.¹⁸⁻²¹ The polaron theory has also been employed to study the quantum transport in the strong coupling regime,²²⁻²⁸ in which strong phonon blockade effect is observed. The polaron transformation extends the validity of perturbative treatment of electron-phonon interaction to strong coupling regime, provided that the electronic couplings are small compared to the typical electron-phonon coupling and bath frequency. However, when this condition is not fulfilled, the polaron theory performs worse than the standard per-

turbative approaches as the polaron cannot follow the system motion accurately.

In order to overcome this shortcoming of polaron transformation based approaches, the variational method has been developed as a generalized polaron transformation.²⁹⁻³³ In contrast with full polaron transformation, the variational polaron approach searches for an optimal amount of transformation by employing variational principle, which is implemented by minimization of the Feynman-Bogolubov upper bound of free energy.³² The optimal transformation is determined by the properties of the bath and system-bath coupling. Thanks to the variational principle, the variational polaron method is able to interpolate between the weak and strong coupling regimes and to capture the dynamic behaviour at arbitrary parameter space. Moreover, compared to the many-body approaches, variational polaron method is computationally economic.

Inspired by the recently developed variational polaron master equation,^{29,30} variational polaron method for dissipative quantum transport is developed in this work, which aims at handling the dissipative quantum transport at arbitrary electron-phonon coupling strength. The manuscript is organized as follows. Sec. II introduces the variational polaron theory for quantum transport and minimization method for determining the optimal parameters for variational transformation. Starting from the variational polaron transformation, the transformed Hamiltonian is divided into two parts: a mean-field part and interacting part. Free energy optimization ends up with an optimal mean-field Hamiltonian and a small interacting perturbation. Then 2PT is applied to establish the quantum transport theory. The variational polaron theory for quantum transport is applied to study the quantum transport through a single site model with different electron-phonon coupling strength, which is given in Sec. IV. Finally, Sec. V summarizes the method developed in this work.

II. VARIATIONAL POLARON THEORY FOR QUANTUM TRANSPORT

A. Model Hamiltonian

Considering a system sandwiched between two leads. The electrons can transfer from one lead to the other through the system driven by bias voltage. The electrons can be scattered inelastically by phonons when transport through the system. The corresponding Hamiltonian reads

$$H = H_S + \sum_{\alpha} [H_{\alpha} + H_{S\alpha}] + H_B + H_{SB}, \quad (1)$$

where H_S is the Hamiltonian of the system; H_B is the Hamiltonian of phonon bath; H_{α} is the Hamiltonian of lead α . The lead serves as electronic bath; H_{SB} and $H_{S\alpha}$ are the Hamiltonians of system-phonon coupling and system-lead interaction, respectively. Expressions of those Hamiltonians are

$$\begin{aligned} H_S &= \sum_n \epsilon_n c_n^{\dagger} c_n, \\ H_{\alpha} &= \sum_{k_{\alpha}} \epsilon_{k_{\alpha}} c_{k_{\alpha}}^{\dagger} c_{k_{\alpha}}, \\ H_{S\alpha} &= \sum_{n, k_{\alpha}} [V_{k_{\alpha}n} c_{k_{\alpha}}^{\dagger} c_n + \text{H.c.}], \\ H_B &= \sum_{n, k} \omega_{n, k} b_{n, k}^{\dagger} b_{n, k}, \\ H_{SB} &= \sum_{n, k} g_{n, k} c_n^{\dagger} c_n (b_{n, k}^{\dagger} + b_{n, k}). \end{aligned} \quad (2)$$

Where ϵ_n denotes the single-particle energy of the electronic state n in the device and c_n^{\dagger} (c_n) is the corresponding creation (annihilation) operator. Similarly, $\epsilon_{k_{\alpha}}$ and $c_{k_{\alpha}}^{\dagger}$ ($c_{k_{\alpha}}$) represent the single-particle energy and creation (annihilation) operator of k th electronic state in lead α , respectively. $V_{k_{\alpha}n}$ is the system-lead coupling strength. The phonon creation and annihilation operators are represented by $b_{n, k}^{\dagger}$ and $b_{n, k}$. And $\omega_{n, k}$ and $g_{n, k}$ are the corresponding phonon energy and electron-phonon coupling constant.

In the absence of electron-phonon coupling, an exact time-dependent quantum transport theory has been developed recently.^{34–38} In presence of electron-phonon coupling, electron has the probability of being scattered inelastically by phonon. Previous theoretical studies of dissipative quantum transport usually focus on two different regimes: weak or strong electron-phonon coupling. In the weak coupling regime, 2PT (or lowest order expansion) is widely employed. While in the strong electron-phonon coupling limit, the electron is localized by phonon scattering. At this regime, polaron theory is suitable for describing the phenomena. In this manuscript, a generalized theory for dissipative quantum transport with arbitrary electron-phonon coupling is developed by extending the polaron theory to its variational version.

B. Variational polaron transformation

Similar to the polaron theory, the variational polaron theory starts from an unitary transformation generated by the operator

$$U = \exp \left[\sum_{n, k} \lambda_{n, k} c_n^{\dagger} c_n (b_{n, k}^{\dagger} - b_{n, k}) \right], \quad (3)$$

where $\lambda_{n, k} = f_{n, k} / \omega_{n, k}$. The unitary operator displaces the phonon oscillation in the positive and negative direction. The parameter $f_{n, k}$ determines the magnitude of the displacement for each mode. It is obvious that $f_{nk} = g_{nk}$ corresponds to the conventional polaron transformation, while $f_{nk} = 0$ denotes no transformation.

After the unitary transformation, the Hamiltonian of the system becomes

$$\bar{H}_S = \sum_n (\epsilon_n + R_n) c_n^{\dagger} c_n, \quad (4)$$

where $R_n = \lambda_{n, k} (f_{n, k} - 2g_{n, k})$ is the renormalization energy which describes the shift of single-particle energy of electronic states induced by electron-phonon interaction. \bar{H}_{α} is same as H_{α} since it commutes with the unitary operator U . While, the system-lead coupling Hamiltonian becomes

$$\bar{H}_{S\alpha} = \sum_{n k_{\alpha}} [V_{k_{\alpha}n} c_{k_{\alpha}}^{\dagger} c_n X_n + \text{H.c.}] \quad (5)$$

after the transformation, i.e., the system-lead coupling is dressed by phonon displacement operator X_n , where X_n is defined as

$$X_n = \exp \left[- \sum_k \lambda_{n, k} (b_{n, k}^{\dagger} - b_{n, k}) \right]. \quad (6)$$

After the unitary transformation, the Hamiltonian of electron-phonon coupling becomes

$$\bar{H}_{SB} = \sum_{n, k} \bar{g}_{n, k} c_n^{\dagger} c_n (b_{n, k}^{\dagger} + b_{n, k}), \quad (7)$$

where $\bar{g}_{n, k} = g_{n, k} - f_{n, k}$ is defined as the reduced electron-phonon coupling strength. $\bar{g}_{n, k}$ indicates that the electron-phonon coupling is reduced by the unitary transformation. In summary, after the variational polaron transformation, phonon's influence on electrons is transferred into three terms: (1) the polaron shift energy R_n , which represents the energy renormalization effect due to electron-phonon interaction; (2) in the dressed coupling between system and leads, the system-lead coupling is renormalized by the displacement operator X_n ; (3) reduced electron-phonon coupling $\bar{g}_{n, k}$, which is zero in the strong coupling limit and approaches g_{nk} in the weak coupling limit.

The variational transformation results in a new kind of system-lead coupling, which is mediated by the phonon

displacement operator. The displacement operator can be divided into two parts:

$$X_n = X_n - \langle X_n \rangle + \langle X_n \rangle \equiv B_n + \langle X_n \rangle,$$

i.e., the expectation value and corresponding fluctuation around its expectation. Assuming phonon is in thermal equilibrium, $\langle X_n \rangle$ can be written as

$$\langle X_n \rangle = \exp \left[-\frac{1}{2} \sum_k \lambda_{n,k}^2 \coth(\beta \omega_{n,k}/2) \right], \quad (8)$$

where β is the inverse temperature. Consequently, $H_{S\alpha}$ can be separated into two parts,

$$\begin{aligned} \bar{H}_{S\alpha}^0 &= \sum_{n,k_\alpha} [V_{k_\alpha n}^R c_{k_\alpha}^\dagger c_n + \text{H.c.}], \\ \bar{H}_{S\alpha}^I &= \sum_{n,k_\alpha} [V_{k_\alpha n} c_{k_\alpha}^\dagger c_n B_n + \text{H.c.}]. \end{aligned} \quad (9)$$

where $V_{k_\alpha n}^R = V_{k_\alpha n} \langle X_n \rangle$ is the renormalized system-lead coupling mediated by phonon. Thus, the total transformed Hamiltonian can also be grouped into two parts. One part is the mean-field (or non-interacting) part \bar{H}_0 and the other one is the interacting Hamiltonian \bar{H}_I , where \bar{H}_0 is defined as

$$\bar{H}_0 = \bar{H}_S + \sum_\alpha (\bar{H}_{S\alpha}^0 + \bar{H}_\alpha) + \bar{H}_B \equiv \bar{H}_e + \bar{H}_B. \quad (10)$$

and \bar{H}_I is

$$\bar{H}_I = \bar{H}_{SB} + \sum_\alpha \bar{H}_{S\alpha}^I. \quad (11)$$

It is obvious that the polaron transformation ($f_{n,k} = g_{n,k}$) makes the electron-phonon interaction term \bar{H}_{SB} vanished. In contrast, the variational polaron transformation employs f_{nk} as parameters and the values of which are determined by the minimization of an upper bound of free energy. The minimization inherent to variational approach allows to minimize the effect of \bar{H}_I and obtain an optimal mean-field Hamiltonian \bar{H}_0 . Thus, given arbitrary electron-phonon coupling strength, the variational polaron transformation in principle can end up with small \bar{H}_I . Consequently, 2PT can be employed to account the effect of \bar{H}_I . Because of the single-particle nature of \bar{H}_0 and second-order perturbative treatment of \bar{H}_I , variational polaron theory significantly reduces the computational complexity compared to the many-particle approaches.

C. Minimization of the upper bound of free energy

In this work, the Feynman-Bogoliubov upper bound of free energy³² is chosen to determine the optimal value of f_{nk} for the variational transformation. The upper bound of free energy is given as

$$F_u = -\frac{1}{\beta} \ln \{ \text{tr} [e^{-\beta \bar{H}_0}] \} + \langle \bar{H}_I \rangle_{\bar{H}_0}, \quad (12)$$

where $\langle \bar{H}_I \rangle_{\bar{H}_0} = \text{Tr} [\bar{H}_I e^{-\beta \bar{H}_0}]$. F_u gives the upper bound of the true free energy F , which is related to F by the inequality $F \leq F_u$. It is obvious that the second term on the right hand right (RHS) of Eq.(12) is zero by the construction. Besides, because $[\bar{H}_B, \bar{H}_e] = 0$, F_u can be further simplified and divided into two parts

$$F_u = F_B - \frac{1}{\beta} \ln \{ \text{tr} [e^{-\beta \bar{H}_e}] \}, \quad (13)$$

where F_B is the free energy of phonon bath. Because F_B is not a function of f_{nk} , it is neglected in the minimization procedure. There are two ways to minimize the upper bound of free energy with respect to f_{nk} . One way is to treat the system and leads as a whole system and the upper bound of free energy can be numerically calculated by the diagonalization of \bar{H}_e . The other approach is to employ the Linked cluster expansion method.³⁹

The mean-field part of the transformation Hamiltonian, \bar{H}_0 , is a function of the phonon-induced renormalization parameters $\{R_n, \langle X_n \rangle\}$. Consequently, the Feynman-Bogoliubov upper bound of free energy F_u can be minimized with respect to $\{R_n, \langle X_n \rangle\}$. Hence, the minimization condition can be written as

$$\frac{dA_S}{df_{n,k}} = \frac{\partial A_S}{\partial R_n} \frac{\partial R_n}{\partial f_{n,k}} + \frac{\partial A_S}{\partial \langle X_n \rangle} \frac{\partial \langle X_n \rangle}{\partial f_{n,k}} = 0. \quad (14)$$

Using the expressions for $\{R_n, \langle X_n \rangle\}$, we can evaluate the derivatives of $\{R_n, \langle X_n \rangle\}$ with respect to $f_{n,k}$ analytically. After simple algebra, the minimization condition gives the expression of the variational transformation parameter $f_{n,k}$ as $f_{n,k} = g_{n,k} F_{n,k}$, where

$$F_{n,k} = \frac{\omega_{n,k} \frac{\partial A_S}{\partial R_n}}{\omega_{n,k} \frac{\partial A_S}{\partial R_n} - \frac{1}{2} \frac{\partial A_S}{\partial \langle X_n \rangle} \coth(\beta \omega_{n,k}/2) \langle X_n \rangle}. \quad (15)$$

Since $\{R_n, \langle X_n \rangle\}$ are also functions of f_{nk} , above equation must be solved self-consistently. After the minimization procedure, the optimal choice of \bar{H}_0 is obtained, resulting in a small \bar{H}_I . Hence, \bar{H}_I can be treated by 2PT. Next, dissipative quantum transport formalism with variational polaron transformation is presented.

III. DISSIPATIVE QUANTUM TRANSPORT THEORY WITH VARIATIONAL POLARON TRANSFORMATION

Non-equilibrium Green's function (NEGF) formalism is employed to study the dissipative quantum transport. The key quantity in the NEGF method is the single-particle Green's function, which is given by

$$\begin{aligned} G_{ij}(\tau, \tau') &= -i \langle T_c c_i(\tau) c_j^\dagger(\tau') \rangle_H \\ &= -i \langle T_c c_i(\tau) X_i(\tau) c_j^\dagger(\tau') X_j^\dagger(\tau') \rangle_{\bar{H}}, \end{aligned} \quad (16)$$

where H and \bar{H} are the Hamiltonians before and after the variational polaron transformation, respectively. τ and

τ' are the time variables defined on the Keldysh contour and T_c is the contour time-ordering operator. Eq.(16) determines the dynamics of the coupled electrons and phonons. We employ the following approximation to decouple the electron and phonon dynamics

$$G_{ij}(\tau, \tau') = \bar{G}_{ij}(\tau, \tau') K_{ij}(\tau, \tau'), \quad (17)$$

where

$$\begin{aligned} \bar{G}_{ij}(\tau, \tau') &= -i \langle T_c c_i(\tau) c_j^\dagger(\tau') \rangle_{\bar{H}} \\ K_{ij}(\tau, \tau') &= \langle T_c X_i(\tau) X_j^\dagger(\tau') \rangle_{\bar{H}}. \end{aligned} \quad (18)$$

The decoupling in Eq.(17) is inherent in the Born-Oppenheimer approximation. Even the decoupling approximation is made, there is still correlation between electron and phonon if self-consistent procedure is operated,²⁶ which is similar to the diagram dressing process in the standard many-body perturbation theory.

With the decoupling approximation, the key quantity becomes $\bar{G}(\tau, \tau')$ which is associated with \bar{H} . As illustrated in Sec. II, the variational polaron transformed Hamiltonian can be divided into two parts: \bar{H}_0 and \bar{H}_I . \bar{H}_0 is mean-field part of the Hamiltonian, the quantum transport problem associated with \bar{H}_0 can be easily solved as demonstrated by previous publications.⁴⁰ While the correction of \bar{H}_I to the quantum transport can be taken into consideration by the perturbation theory since the variational polaron transformation in principle ends up with small \bar{H}_I . Firstly, zero-order Green's function $G_0(\tau, \tau')$ is obtained by using \bar{H}_0 ,

$$\begin{aligned} G_0(\tau, \tau') &= g_0(\tau, \tau') + \int d\tau_1 \int d\tau_2 g_0(\tau, \tau_1) \\ &\quad \times \left[\sum_{\alpha} \bar{\Sigma}_{0\alpha}(\tau_1, \tau_2) \right] G_0(\tau_2, \tau'), \end{aligned} \quad (19)$$

where $g_0(\tau, \tau')$ is the electron Green's function in absence of system-lead coupling. The effect of system-lead coupling is represented by the self-energy

$$\begin{aligned} \bar{\Sigma}_{0\alpha,ij}(\tau, \tau') &= \sum_{k_{\alpha}} V_{k_{\alpha}i}^* V_{k_{\alpha}j} g_{k_{\alpha}}(\tau, \tau') \langle X_i \rangle \langle X_j \rangle \\ &= \Sigma_{\alpha,ij}(\tau, \tau') \langle X_i \rangle \langle X_j \rangle, \end{aligned} \quad (20)$$

where $g_{k_{\alpha}}(\tau, \tau')$ is the surface Green's function of lead α and $\Sigma_{\alpha}(\tau, \tau')$ is the lead self-energy in absence of phonon renormalization. Next, $G(\tau, \tau')$ is derived at second-order expansion with respect to \bar{H}_I , starting from $G_0(\tau, \tau')$.

A. Second-order perturbation theory

Within the 2PT theory, the Green's function can be expressed as

$$\begin{aligned} \bar{G}(\tau, \tau') &= \bar{G}_0(\tau, \tau') + \int d\tau_1 \int d\tau_2 \bar{G}_0(\tau, \tau_1) \\ &\quad \times \bar{\Sigma}_I(\tau_1, \tau_2) \bar{G}_0(\tau_2, \tau'), \end{aligned} \quad (21)$$

where $\bar{\Sigma}_I(\tau, \tau')$ is the self-energy to Green's function at the second-order with respect to \bar{H}_I and $\bar{G}_0(\tau, \tau')$ is the Green's function corresponding to \bar{H}_0 . Since \bar{H}_I contains two parts, $\bar{H}_{S\alpha}^I$ and \bar{H}_{SB} , $\bar{\Sigma}_I(\tau, \tau')$ can also be divided into two parts accordingly,

$$\bar{\Sigma}_I(\tau, \tau') = \bar{\Sigma}_{ep}(\tau, \tau') + \sum_{\alpha} \bar{\Sigma}_{I\alpha}(\tau, \tau').$$

Within the 2PT, $\Sigma_I(\tau, \tau')$ is derived as

$$\begin{aligned} \bar{\Sigma}_{I\alpha,ij}(\tau, \tau') &= \sum_{k_{\alpha}} V_{k_{\alpha}i}^* V_{k_{\alpha}j} g_{k_{\alpha}}(\tau, \tau') \\ &\quad \times \langle T_C B_j(\tau') B_i^\dagger(\tau) \rangle_{\bar{H}_0}. \end{aligned} \quad (22)$$

The definition of $\bar{\Sigma}_{I\alpha}$ is very similar to Eq.(20) except the phonon renormalization factor $\langle X_i \rangle$ is replaced by the correlation function of B_i . According to the definition of B_i , the self-energy $\Sigma_{\alpha,I}$ can be rewritten as

$$\begin{aligned} \bar{\Sigma}_{I\alpha,ij}(\tau, \tau') &= \Sigma_{\alpha,ij}(\tau, \tau') [K_{ji}(\tau', \tau) - \langle X_i \rangle \langle X_j \rangle] \\ &= \Sigma_{\alpha,ij}(\tau, \tau') K_{ji}(\tau', \tau) - \bar{\Sigma}_{0\alpha,ij}(\tau, \tau') \end{aligned} \quad (23)$$

where $\bar{\Sigma}_{0\alpha}(\tau, \tau')$ is the phonon dressed self-energy, which is used to evaluate the zero-order Green's function $\bar{G}_0(\tau, \tau')$ as described previously.

The derivation of $\bar{\Sigma}_{ep}(\tau, \tau')$ is same as that in Ref. 6. The only difference is that the electron-phonon coupling constant ($g_{n,k}$) is replaced by the reduced one ($\bar{g}_{n,k}$). The expression of $\bar{\Sigma}_{ep}(\tau, \tau')$ is

$$\Sigma_{ep}(\tau, \tau') = \sum_{n,k} \bar{g}_{n,k} D_0(\tau, \tau') \bar{G}_0(\tau, \tau') \bar{g}_{n,k}, \quad (24)$$

where $D_0(\tau, \tau')$ is the bare phonon Green's function.

In practical implementation, the Green's function and self-energies defined on the Keldysh contour are projected on real axis, resulting in equations for retarded/advanced and lesser/greater Green's functions and self-energies. In this work, we focuses on the steady state. In steady state, all quantities (two-time functions) are only dependent on the time difference instead of two times. Hence, Fourier transformation is employed to transfer the quantities from real-time domain to energy space. Since \bar{H}_0 is the mean-field part of the total Hamiltonian, the corresponding Green's functions can be easily evaluated,

$$\begin{aligned} \bar{G}_0^r(E) &= [E + i\eta - \bar{H}_0 - \sum_{\alpha} \bar{\Sigma}_{0\alpha}^r(E)]^{-1}, \\ \bar{G}_0^<(E) &= \bar{G}_0^r(E) [\sum_{\alpha} \bar{\Sigma}_{0\alpha}^<(E)] \bar{G}_0^a(E), \end{aligned} \quad (25)$$

where $\eta \rightarrow 0^+$. $\bar{\Sigma}_{0\alpha}^r$ and $\bar{\Sigma}_{0\alpha}^<$ are phonon dressed retarded and lesser self-energies of lead α , respectively, which are written as

$$\begin{aligned} \bar{\Sigma}_{\alpha,ij}^{r/<}(E) &= \sum_{k_{\alpha}} V_{ik_{\alpha}}^* V_{k_{\alpha}j} g_{k_{\alpha}}^{r/<}(E) \langle X_i \rangle \langle X_j \rangle \\ &= \Sigma_{\alpha,ij}^r(E) \langle X_i \rangle \langle X_j \rangle \end{aligned} \quad (26)$$

Defining the unperturbed line-width function as $\Gamma_\alpha(E) = -2\Im[\Sigma_\alpha^r(E)]$, where \Im denotes the imaginary part. Thus, the phonon dressed line-width function becomes $\bar{\Gamma}_{\alpha,ij}(E) = \Gamma_{\alpha,ij}(E)\langle X_i \rangle \langle X_j \rangle$. The dressing factor indicates the localization of electron induced by the electron-phonon interaction. In term of line-width function, the corresponding lesser self-energy can be rewritten as $\bar{\Sigma}_\alpha^{r/<}(E) = if_\alpha(E)\bar{\Gamma}_\alpha(E)$ according to the fluctuation-dissipation law, where $f_\alpha(E)$ is the Fermi-Dirac distribution function of lead α with chemical potential μ_α .

After obtaining the zeroth-order Green's functions, $\bar{G}_0^{r/<}(E)$, are evaluated, the Green's function with \bar{H}_I is obtained from the 2PT theory as

$$\begin{aligned}\bar{G}^r(E) &= \bar{G}_0^r(E) + \bar{G}_0^r(E)\bar{\Sigma}_I^r(E)\bar{G}_0^r(E), \\ \bar{G}^{r/<}(E) &= \bar{G}_0^{r/<}(E) + \bar{G}_0^r(E)\bar{\Sigma}_I^{r/<}(E)\bar{G}_0^{r/<}(E).\end{aligned}\quad (27)$$

where $\bar{\Sigma}_I^{r/<}(E)$ is the self-energy to Green's function at the second-order with respect to \bar{H}_I . As shown previously, $\bar{\Sigma}_I^{r/<}(E)$ contains two parts,

$$\bar{\Sigma}_I^{r/<}(E) = \bar{\Sigma}_{ep}^{r/<}(E) + \sum_\alpha \bar{\Sigma}_{I\alpha}^{r/<}(E).$$

Retarded and lesser phonon self-energies within the 2PT are^{6,41,42}

$$\begin{aligned}\bar{\Sigma}_{ep}^{r/<}(E) &= \sum_{q,\pm} \bar{g}_q N_q^\pm \bar{G}_0^{r/<}(E \pm \omega_q) \bar{g}_q, \\ \bar{\Sigma}_{ep}^r(E) &= \sum_{q,\pm} \bar{g}_q [N_q^\mp \bar{G}_0^r(E \pm \omega_q) \pm \bar{G}_0^{r/<}(E \mp \omega_q)] \bar{g}_q\end{aligned}\quad (28)$$

where $N_q^\pm = N_q + \frac{1}{2} \pm \frac{1}{2}$. N_q is the phonon occupation number of mode q , which is determined by Bose-Einstein distribution function.

The derivation of $\bar{\Sigma}_{I\alpha}^{r/<}(E)$ requires the knowledge of the displacement correlation function $K(\tau, \tau')$, which is nontrivial. $K(\tau, \tau')$ in principle depends on the phonon Green's function which is coupled with electronic Green's function via its self-energy.²⁶⁻²⁸ Therefore, self-consistent calculation of phonon and electron Green's function is required. However numerical implementation of self-consistent calculation is non-trivial and very computational demanding. In practise, we assume the phonon is in equilibrium and undressed by the electron in this work. The influence of electron to the phonon can be introduced through a phenomenological rate equation including the renormalization, damping and heating effect.⁴³⁻⁴⁵ With the assumption that phonon is in the equilibrium and undressed by electron, the displacement correlation function can be rewritten in a simple form.^{24,26,39} The lesser projection of displacement correlation function is expressed as

$$\begin{aligned}K_{ij}^{r/<}(t, t') &= \langle X_j^\dagger(t') X_i(t) \rangle. \\ &= \prod_{q=1} \left\{ e^{-\frac{\lambda_{iq}^2 + \lambda_{jq}^2}{2} (2N_q + 1)} \exp \left\{ \lambda_{iq} \lambda_{jq} \times \right. \right. \\ &\quad \left. \left. [N_q e^{-i\omega_q(t-t')} + (N_q + 1) e^{i\omega_q(t-t')}] \right\} \right\}\end{aligned}\quad (29)$$

where N_q is the occupation number for the q th phonon mode. $K_{ij}^{r/<}(t, t')$ can be decomposed as

$$\begin{aligned}K_{ij}^{r/<}(t, t') &= \prod_{q=1}^M \left[\sum_{p_q} L_{ij}^{p_q} e^{ip_q \omega_q (t-t')} \right] \\ &= \sum_{p_1 p_2 \dots p_M} L_{ij}^{p_1} L_{ij}^{p_2} \dots L_{ij}^{p_M} e^{i\mathbf{p}^T \boldsymbol{\omega} (t-t')} \\ &\equiv \sum_{\mathbf{p}} L_{ij}^{\mathbf{p}} e^{i\mathbf{p}^T \boldsymbol{\omega} (t-t')},\end{aligned}\quad (30)$$

where both \mathbf{p} and $\boldsymbol{\omega}$ are row vectors, $\mathbf{p}^T \boldsymbol{\omega} = \sum_q p_q \omega_q$. And $L_{ij}^{\mathbf{p}} = L_{ij}^{p_1} L_{ij}^{p_2} \dots L_{ij}^{p_M}$, where $L_{ij}^{p_q}$ is modified Bessel function

$$\begin{aligned}L_{ij}^{p_q} &= e^{-\frac{\lambda_{iq}^2 + \lambda_{jq}^2}{2} (2N_q + 1)} e^{p_q \omega_q \beta/2} \\ &\times I_{p_q} \left[2\lambda_{iq} \lambda_{jq} \sqrt{N_q(N_q + 1)} \right],\end{aligned}\quad (31)$$

and I_{p_q} is the p_q th order Bessel function.

The greater projection of displacement correlation function is $K_{ij}^{>}(t, t') = \langle X_i(t) X_j^\dagger(t') \rangle = [K_{ij}^{r/<}(t, t')]^\dagger$. It can be verified that $K^{<}(t, t') \simeq K^{>}(t, t')$ in the high-temperature limit since $N_q \simeq N_q + 1$ in this limit. Actually, many works even adopt $K^{<}(t, t') \simeq K^{>}(t, t')$ as an approximation in low temperature, which is regarded as neglecting the Fermi Sea.^{22-25,46}

With $K^{<}/>(t, t')$ known, the lesser (greater) self-energy in energy space can be obtained from the Fourier transformation of $\Sigma_{I\alpha}^{<}/>(t, t')$,

$$\begin{aligned}\bar{\Sigma}_{I\alpha,ij}^{r/<}(E) &= \sum_{\mathbf{p}} L_{ji}^{\mathbf{p}} \Sigma_{\alpha,ij}^{r/<}(E - \mathbf{p}^T \boldsymbol{\omega}) - \bar{\Sigma}_{0\alpha,ij}^{r/<}(E), \\ \bar{\Sigma}_{I\alpha,ij}^{>}(E) &= \sum_{\mathbf{p}} L_{ji}^{\mathbf{p}} \Sigma_{\alpha,ij}^{>}(E + \mathbf{p}^T \boldsymbol{\omega}) - \bar{\Sigma}_{0\alpha,ij}^{>}(E).\end{aligned}\quad (32)$$

B. Observable of interest

The steady-state current through the junction can be expressed in Meir-Wingreen formula⁴⁰

$$I_\alpha = \frac{2e}{\hbar} \int \frac{dE}{2\pi} T_\alpha(E) \quad (33)$$

where the factor 2 accounts for the spin degeneracy and T_α is the transmission coefficient through lead α , which is expressed in terms of Green's functions and self-energies within NEGF formalism

$$T_\alpha(E) = \text{Tr} [\Sigma_\alpha^{r/<}(E) G^>(E) - \Sigma_\alpha^{>}(E) G^{r/<}(E)]. \quad (34)$$

As shown in Eq.(17), lesser/greater projection of Green's functions are

$$G_{ij}^{r/<}(t, t') = \bar{G}_{ij}^{r/<}(t, t') K_{ij}^{r/<}(t, t').$$

Utilizing the expansion of $K_{ij}^{\lessgtr}(t, t')$, Fourier transformation of above equations gives the Green's functions as

$$\begin{aligned} G_{ij}^>(E) &= \sum_{\mathbf{p}} L_{ij}^{\mathbf{p}} \bar{G}_{ij}^>(E - \mathbf{p}^T \boldsymbol{\omega}), \\ G_{ij}^<(E) &= \sum_{\mathbf{p}} L_{ij}^{\mathbf{p}} \bar{G}_{ij}^<(E + \mathbf{p}^T \boldsymbol{\omega}). \end{aligned} \quad (35)$$

Hence, transmission coefficient and current can be obtained through substituting Eq.(35) into Eq.(34).

In short, the computational procedures are summarized as follows: (1) Firstly, bare Green's functions $\bar{G}_0^{r,\lessgtr}(E)$ in variational polaron picture are calculated; (2) Secondly, Green's functions $\bar{G}^{r,\lessgtr}(E)$ at the second-order with respect to \bar{H}_I are evaluated; (3) Thirdly, Green's functions in the H picture are obtained through Eqs.(35); (4) Finally, physical quantities, such as density of states (DOS) and currents, are obtained from the Green's functions and self-energies.

IV. NUMERICAL EXAMPLES

The variational polaron theory for dissipative quantum transport is employed to study the transport through on a monoatomic chain. The system consists of a single site. The two leads are modeled by semi-infinite linear chains as illustrated in Fig. 1. The onsite energy of the system is denoted by ϵ_S . The onsite energy and hopping element of leads are ϵ and t , respectively. The system-lead coupling constant is denoted by V_α . In this work, it is assumed that the system is coupled to the two leads equally, i.e., $V_L = V_R = v$. The line-width function of the semi-infinite tight-binding lead can be evaluated analytically⁴⁷

$$\Gamma_\alpha(E) = V_\alpha^2 \frac{\sqrt{4t^2 - (E - \mu_\alpha)^2}}{t^2}, \quad (36)$$

where μ_α is the chemical potential of lead α .

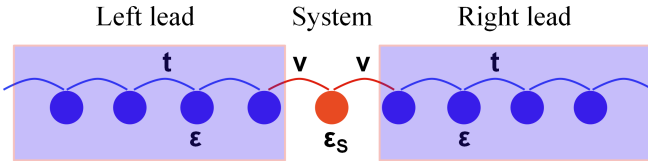


FIG. 1. Illustration of a single site model coupled to two leads. It is assumed that the system coupled to the two lead equally, which is denoted by v . The onsite energy and hopping element of leads are ϵ and t , respectively.

In this work, the system-lead coupling is set to be equal to the hopping in the leads, i.e., $v = t$. The onsite energy is set to be 0 eV and hopping is set as $t = 0.1$ eV. And the Fermi energy of the leads is 0 eV, which corresponds to half-filled on each site. Temperature is set as $T = 300$ K. In this work, only one phonon mode is considered to be coupled to the system for simplification. The optimal

value f of variational polaron transformation is searched for different phonon frequency and electron-phonon coupling strength. The phonon frequency is chosen in three different regimes: $\omega > t$, $\omega = t$ and $\omega < t$. The optimal value f of variational polaron transformation for different electron-phonon coupling constant g is shown in Fig. 2. As it is expected, different electron-phonon coupling strength corresponds to different optimal value of f in the variational transformation. Besides, f increases monotonously with electron-phonon coupling strength g . When $g \rightarrow 0$, f/g ratio approaches a small value which is affected by the phonon energy. In the $g \rightarrow 0$ limit, f/g ratio is small, which is close to no polaron transformation. While in the strong electron-phonon coupling limit ($g \rightarrow \infty$), f/g ratio approaches to 1, which corresponds to full polaron transformation. In the intermediate regime, variational polaron transformation ends up with $f/g < 1$, which denotes the partial polaron transformation.

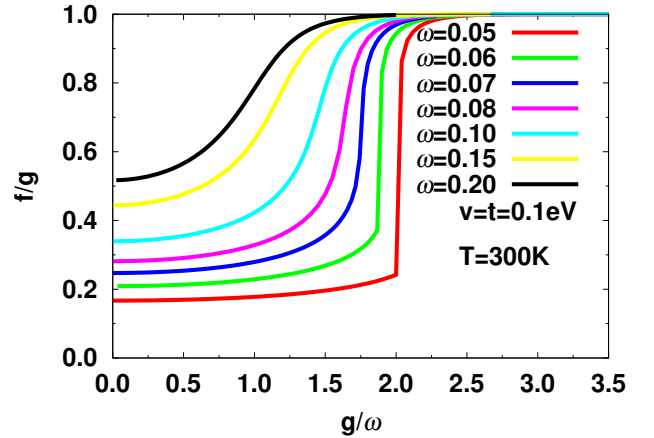


FIG. 2. Optimal value f of variational polaron transformation against different electron-phonon coupling constant g . Parameters are: The system-lead coupling and hopping in leads are $v = t = 0.1$ eV; $T = 300$ K.

It is also noticed from Fig. 2 that there is a shape transition of f in a certain regime of g if $\omega < t$. Larger $\frac{t}{\omega}$ results in the steeper transition. Finally, f shows discontinuity against $\frac{g}{\omega}$. This discontinuity appears because different local minimum becomes the global minimum at certain parameter regime. Taking $\omega = 0.05$ eV as example, the free energies against f/g ratio with electron-phonon coupling strength around 0.1 eV are plotted in Fig. 3. As it shown by Fig. 3, two local minimums start to emerge at $g \approx 0.1$ eV. The local minimums of smaller and larger f/g become the global minimum for $g = 0.098$ eV and $g = 0.102$ eV, respectively. The discontinuity of f may cause unphysical phase transition from delocalized to localized regime.^{33,48,49} For multiple sites systems, the free energy can be more complex and more local minimums may emerge, thus there is larger possibility of discontinuity. However, even the discontinuity appears, the variational transformation is still likely to work better

than the untransformed scheme or polaron transformation. Moreover, the discontinuity of f may be removed by employing certain ansatz. For instance, a ground state ansatz has been proposed recently to get rid of the discontinuity in the variational polaron.^{49,50} Similar ansatz may be proposed to remove the discontinuity problem in the quantum transport system, which is the scope of further improvement of the method.

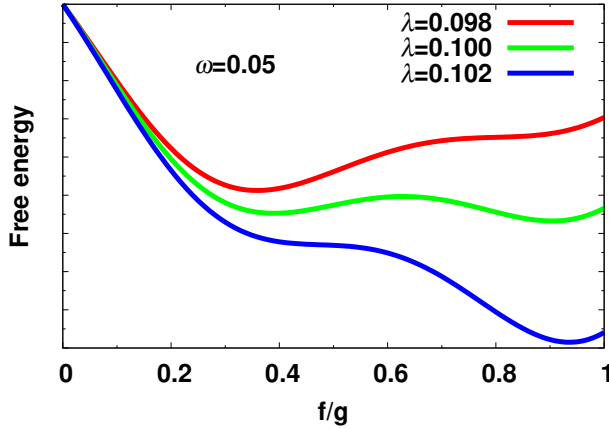


FIG. 3. Free energy as function of variational transformation parameter f for different electron-phonon coupling strength g . The phonon energy is 0.05 eV. When g is around 0.10 \sim 0.102 eV, different local minimum may become the global minimum, resulting in abrupt transition of f .

After the variational polaron transformation is found, the quantum transport properties of the system, such as DOS and current-voltage characteristics, at different electron-phonon coupling regime can be studied by the method developed in Sec. III. Here, three sets of parameters are studied, ranging from weak to strong electron-phonon coupling regime. The parameters as well as optimal factor of variational polaron transformation are summarized in Table I. Model A and C are in the weak and strong coupling regime, respectively, and Model B is in the moderate coupling regime. The optimal values of variational polaron transformation are 0.17, 0.54 and 0.90. Here, the g/ω ratio is set as a constant for the three models. As shown by Fig. 2, large g/ω ratio ($g/\omega \gg 1$) makes the system in polaron regime while small g/ω ratio ($g/\omega \ll 1$) makes the system in weak or moderate coupling regime. Hence, $g/\omega = 0.8$ is chosen to make sure that the system varies from the weak to strong coupling by tuning the electron-phonon coupling constant.

TABLE I. Parameters of the Models.

Model	ω (eV)	g (eV)	f/g
A	0.05	0.04	0.17
B	0.15	0.12	0.54
C	0.40	0.32	0.90

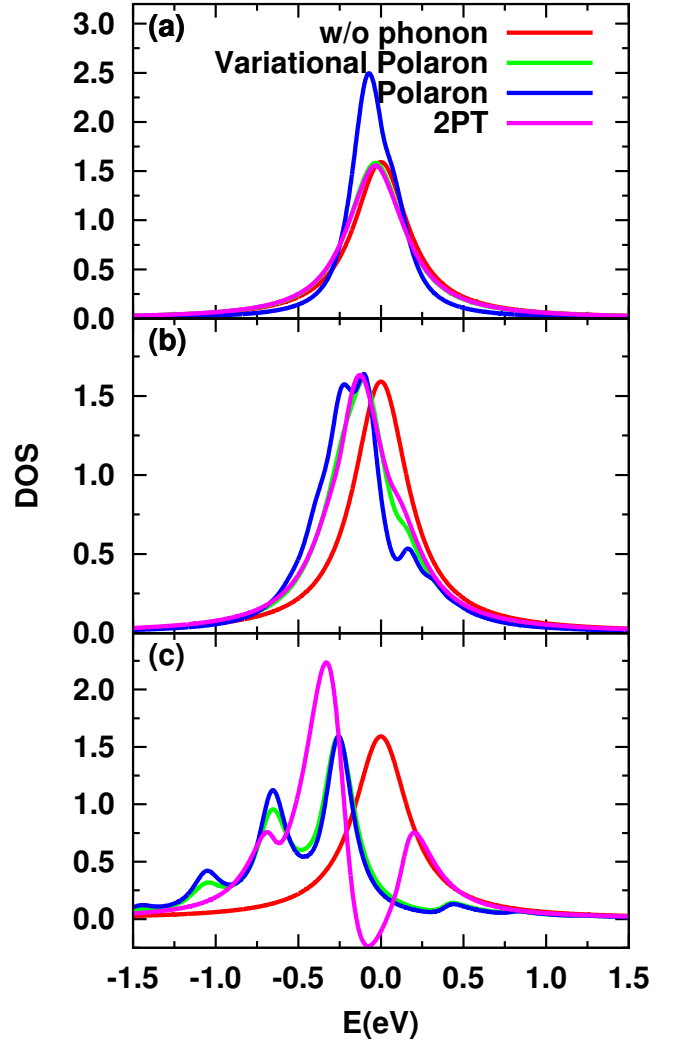


FIG. 4. DOS of the system with different electron-phonon coupling constant: (a) $\omega = 0.05$ eV and $g = 0.04$ eV; The electron-phonon interaction is in the weak coupling regime. DOS of variational polaron is same as that of 2PT, while polaron theory overestimates the phonon side-bands. (b) $\omega = 0.15$ eV and $g = 0.12$ eV; In this moderate electron-phonon coupling regime, 2PT starts to fail and polaron still overestimates the phonon side-bands. (c) $\omega = 0.40$ eV and $g = 0.32$ eV. The system is in the strong coupling regime. Variational polaron theory gives similar results as polaron theory does. While 2PT is not applicable to this regime, it even gives unphysical DOS. See text for other parameters.

In presence of electron-phonon coupling, electronic structure of the system is affected at different levels depending on the electron-phonon coupling strength. Consequently, DOS of the system is affected, such effects include energy shift of peak, broadening of the spectral and emergence of phonon side-bands. Fig. 4 plots the DOS of the system with different electron-phonon coupling strength.

(a) In model A, the electron-phonon coupling strength

is small. Phonon has limited effects on the electronic structure of the system. The phonon-induced energy shift is about 50 meV. The DOS of variational polaron transformation is close to that of 2PT. Moreover, the DOS of both variational polaron theory and 2PT is almost the same as that of non-interacting system except the phonon-induced shift of the peak. No obvious phonon side-bands are observed in the DOS of variational polaron theory and 2PT. However, polaron theory overestimates the energy shift and phonon side-bands. Because polaron theory overestimates the phonon dressed system-lead coupling, resulting in stronger localization effect. Consequently, main peak of DOS is sharpened and phonon side-band appears as shown in Fig. 4(a).

(b) In the moderate coupling regime, phonon has larger effect on the electronic structure of the system and phonon side-bands start to appear due to the increased phonon-induced electron localization. In this coupling regime, the DOS of variational polaron theory starts to deviate from that of 2PT as shown by Fig. 4(b). Due to the principle of 2PT, only two phonon side-bands can be observed in the DOS. However, higher order corrections become more and more significant in the moderate coupling regime. As a result, 2PT starts to fail to describe the renormalization effect induced by phonon. Besides the phonon side-bands, the energy shift due to electron-phonon interaction is underestimated slightly by 2PT. In contrast, higher order phonon side-bands can be evaluated by both polaron theory and variational polaron theory. But, polaron theory still overestimates the phonon dressed system-lead coupling compared with variational polaron theory. Consequently, the phonon side-bands are much more significant in the DOS. While, variational polaron theory neither underestimates nor overestimates the renormalization effect. The DOS of variational polaron lies between those of 2PT and polaron.

(c) In the strong coupling limit, phonon induces pronounced side-bands effect and polaron is formed. Consequently, the variational polaron transformation approaches the polaron theory. As shown by Fig. 4(c), DOS of variational polaron theory is almost the same as that of polaron theory since the optimal value of f/g is 0.9, which is close to 1, i.e., variational polaron theory approaches the polaron theory. In the contrast, 2PT greatly underestimates the phonon side-bands and overestimates the phonon-induced energy shift. The pronounced phonon side-bands indicate that electron is localized by the phonon. The phonon side-bands are also responsible for the phonon blockade in the current-voltage characteristics, which is represented by steps in the current-voltage characteristics or peaks in the differential conductance.^{23–26}

V. SUMMARY

In this work, a dissipative quantum transport theory with electron-phonon coupling at arbitrary param-

eter regime is developed by employing the variational polaron transformation. Variational polaron transformation provides an optimal set of parameters for the unitary transformation, which is determined by the minimization of the Feynman-Bogoliubov upper bound of free energy. After the minimization, variational polaron transformation is able to end up with an optimal mean-field Hamiltonian and a small perturbation. The mean-field part Hamiltonian, \bar{H}_0 , contains the phonon-induced energy renormalization and phonon dressed system-lead coupling. Thanks to the variational polaron transformation, the many-body effect of electron-phonon interaction is transformed into the small interacting part of the Hamiltonian (\bar{H}_I), which validates the 2PT treatment. Upon the variational transformation, a quantum transport theory with electron-phonon interaction at arbitrary parameter regime is established within NEGF formalism. Following the quantum transport theory of non-interaction system, the mean-field part is treated exactly. \bar{H}_I is taken into account through the self-energies which are in second-order of \bar{H}_I .

Numerical examples on a monoatomic chain demonstrate the validity of the variational transformation. The optimal value of variational transformation increases monotonously with electron-phonon coupling strength, which connects the 2PT in weak coupling regime and polaron theory in strong coupling limit. Comparison of DOS in different parameter regimes indicates the applicability of variational polaron transformation: (a) In weak coupling limit, polaron theory overestimates the phonon-induced energy shift and side-bands; (b) In the strong coupling limit, 2PT underestimates the renormalization effect induced by phonon and even gives unphysical DOS; (c) Variational polaron transformation naturally connects the 2PT in the weak coupling limit and polaron theory in the strong coupling limit by making use of the optimal transformation. More numerical benchmark comparison with other numerically exact methods, such as QUAPI and MCTDH, will be considered in the future works. Moreover, the sudden change of the optimal value of variational transformation may be solved by employing certain ansatz,^{49,50} which is also the scope of future improvement of the method.

ACKNOWLEDGMENTS

Y. Zhang thanks Jianshu Cao, Weitao Yang, E. K. U. Gross and Garnet Chan for helpful discussions. The support from the Hong Kong Research Grant Council (Contract Nos. HKU7009/09P, 7009/12P, 7007/11P, and HKUST9/CRF/11G (G.H. Chen)), the University Grant Council (Contract No. AoE/P-04/08 (G.H. Chen)), National Natural Science Foundation of China (NSFC 21322306 (C.Y. Yam), NSFC 21273186 (G.H. Chen, C.Y. Yam)), and National Basic Research Program of China (2014CB921402 (C.Y. Yam)) is gratefully acknowledged.

-
- * zhy@yangtze.hku.hk; Present institute: Center of Bio-inspired Energy Science, Northwestern University, Evanston, IL, USA.
- † ghc@everest.hku.hk
- ¹ M. Kumar, R. Avriller, A. L. Yeyati, and J. M. van Ruitenbeek, *Phys. Rev. Lett.* **108**, 146602 (2012).
 - ² N. Agraït, C. Untiedt, G. Rubio-Bollinger, and S. Vieira, *Phys. Rev. Lett.* **88**, 216803 (2002).
 - ³ M. Paulsson, T. Frederiksen, H. Ueba, N. Lorente, and M. Brandbyge, *Phys. Rev. Lett.* **100**, 226604 (2008).
 - ⁴ Y. Dubi and M. Di Ventra, *Rev. Mod. Phys.* **83**, 131 (2011).
 - ⁵ G. Romano, A. Gagliardi, A. Pecchia, and A. Di Carlo, *Phys. Rev. B* **81**, 115438.
 - ⁶ Y. Zhang, C. Y. Yam, and G. H. Chen, *J. Chem. Phys.* **138**, 164121 (2013).
 - ⁷ T. Brixner, J. Stenger, H. M. Vaswani, M. Cho, R. E. Blankenship, and G. R. Fleming, *Nature* **434**, 625 (2005).
 - ⁸ J. Wu, F. Liu, Y. Shen, J. Cao, and R. J. Silbey, *New. J. Phys.* **12**, 105012 (2010).
 - ⁹ M. Cho, H. M. Vaswani, T. Brixner, J. Stenger, and G. R. Fleming, *J. Phys. Chem. B* **109**, 10542 (2005).
 - ¹⁰ M. Galperin, M. A. Ratner, and A. Nitzan, *Nano Lett.* **5**, 125 (2005).
 - ¹¹ H. Park, J. Park, A. K. L. Lim, E. H. Anderson, A. P. Alivisatos, and P. L. McEuen, *Nature* **407**, 57 (2000).
 - ¹² Y. Tanimura, *J. Phys. Soc. Jpn.* **75**, 082001 (2006).
 - ¹³ A. Ishizaki and Y. Tanimura, *J. Phys. Soc. Jpn.* **74**, 3131 (2005).
 - ¹⁴ N. Makri and D. E. Makarov, *J. Chem. Phys.* **102**, 4600 (1995); *J. Chem. Phys.* **102**, 4611 (1995).
 - ¹⁵ M. Beck, A. Jäckle, G. Worth, and H.-D. Meyer, *Phys. Rep.* **324**, 1 (2000).
 - ¹⁶ M. Thoss, H. Wang, and W. H. Miller, *J. Chem. Phys.* **115**, 2991 (2001).
 - ¹⁷ H.-D. Meyer, U. Manthe, and L. Cederbaum, *Chem. Phys. Lett.* **165**, 73 (1990).
 - ¹⁸ D. P. S. McCutcheon and A. Nazir, *Phys. Rev. B* **83**, 165101 (2011); *Nwe J. Phys.* **12**, 113042 (2010).
 - ¹⁹ A. Nazir, *Phys. Rev. Lett.* **103**, 146404 (2009).
 - ²⁰ S. Jang, *J. Chem. Phys.* **131**, 164101 (2009); *J. Chem. Phys.* **135**, 034105 (2011).
 - ²¹ S. Jang, Y.-C. Cheng, D. R. Reichman, and J. D. Eaves, *J. Chem. Phys.* **129**, 101104 (2008).
 - ²² N. S. Wingreen, K. W. Jacobsen, and J. W. Wilkins, *Phys. Rev. B* **40**, 11834 (1989).
 - ²³ U. Lundin and R. H. McKenzie, *Phys. Rev. B* **66**, 075303 (2002).
 - ²⁴ Z.-Z. Chen, R. Lü, and B.-F. Zhu, *Phys. Rev. B* **71**, 165324 (2005).
 - ²⁵ J.-X. Zhu and A. V. Balatsky, *Phys. Rev. B* **67**, 165326 (2003).
 - ²⁶ M. Galperin, A. Nitzan, and M. A. Ratner, *Phys. Rev. B* **73**, 045314 (2006).
 - ²⁷ R. Härtle, C. Benesch, and M. Thoss, *Phys. Rev. B* **77**, 205314 (2008); R. Härtle, M. Butzin, and M. Thoss, *Phys. Rev. B* **87**, 085422 (2013).
 - ²⁸ Y. Zhang, C. Y. Yam, and G. H. Chen, *arXiv:1412.5740* (2014).
 - ²⁹ D. P. S. McCutcheon, N. S. Dattani, E. M. Gauger, B. W. Lovett, and A. Nazir, *Phys. Rev. B* **84**, 081305 (2011).
 - ³⁰ F. A. Pollock, D. P. S. McCutcheon, B. W. Lovett, E. M. Gauger, and A. Nazir, *N. J. Phys.* **15**, 075018 (2013).
 - ³¹ D. P. S. McCutcheon and A. Nazir, *J. Chem. Phys.* **135**, 114501 (2011).
 - ³² R. Silbey and R. A. Harris, *J. Chem. Phys.* **80**, 2615 (1984); R. A. Harris and R. Silbey, *J. Chem. Phys.* **83**, 1069 (1985).
 - ³³ C. K. Lee, J. Moix, and J. Cao, *J. Chem. Phys.* **136**, 204120 (2012).
 - ³⁴ X. Zheng, G. H. Chen, Y. Mo, S. Koo, H. Tian, C. Yam, and Y. Yan, *J. Chem. Phys.* **133**, 114101 (2010).
 - ³⁵ X. Zheng, F. Wang, C. Yam, Y. Mo, and G. H. Chen, *Phys. Rev. B* **75**, 195127 (2007).
 - ³⁶ X. Zheng, C. Yam, F. Wang, and G. H. Chen, *Phys. Chem. Chem. Phys.* **13**, 14358 (2011).
 - ³⁷ Y. Zhang, S. Chen, and G. H. Chen, *Phys. Rev. B* **87**, 085110 (2013).
 - ³⁸ H. Xie, F. Jiang, H. Tian, X. Zheng, Y. Kwok, S. Chen, C. Yam, Y. Yan, and G. H. Chen, *J. Chem. Phys.* **137**, 044113 (2012).
 - ³⁹ G. D. Mahan, *Many-particle physics*, 3rd ed. (Kluwer Academic, New York, 2000).
 - ⁴⁰ A.-P. Jauho, N. S. Wingreen, and Y. Meir, *Phys. Rev. B* **50**, 5528 (1994).
 - ⁴¹ Y. Zhang, L. Meng, C. Yam, and G. H. Chen, *J. Phys. Chem. Lett.* **5**, 1272 (2014).
 - ⁴² M. Bescond, C. Li, H. Mera, N. Cavassilas, and M. Lannoo, *J. Appl. Phys.* **114**, 153712 (2013).
 - ⁴³ M. Paulsson, T. Frederiksen, and M. Brandbyge, *Phys. Rev. B* **72**, 201101 (2005).
 - ⁴⁴ T. Frederiksen, M. Brandbyge, N. Lorente, and A.-P. Jauho, *Phys. Rev. Lett.* **93**, 256601 (2004).
 - ⁴⁵ K. Kaasbjerg, T. Novotný, and A. Nitzan, *Phys. Rev. B* **88**, 201405 (2013).
 - ⁴⁶ H. Haug and A.-P. Jauho, *Quantum kinetics in transport and optics of semiconductors* (Springer, 2008).
 - ⁴⁷ E. Scheer, *Molecular Electronics: An Introduction to Theory and Experiment* (World Scientific, 2010).
 - ⁴⁸ D. Yarkony and R. Silbey, *J. Chem. Phys.* **65**, 1042 (1976).
 - ⁴⁹ A. Nazir, D. P. S. McCutcheon, and A. W. Chin, *Phys. Rev. B* **85**, 224301 (2012).
 - ⁵⁰ S. Bera, A. Nazir, A. W. Chin, H. U. Baranger, and S. Florens, *Phys. Rev. B* **90**, 075110 (2014).